Supplementary Material:

Negative and near-zero Poisson's ratio of interlayer space in 2D Graphene/MoS_2 and Graphene/*h*-BN heterostructures

Xiaowen Li[ab], Chuanwei Huang[c], Songbai Hu[b], Bei Deng[b], Zuhuang Chen[d], Wenqiao Han[b] and Lang Chen[*b]

[a]Department of Physics, Harbin Institute of Technology, Harbin 150080, China.

[b]Department of Physics, Southern University of Science and Technology, Shenzhen, Guangdong 518055, China.

[c]Shenzhen Key Laboratory of Special Functional Materials College of Materials Science and Engineering, Shenzhen University, Shenzhen, Guangdong 518060, China.

[d]School of Materials Science and Engineering, Harbin Institute of Technology, Shenzhen, Guangdong 518055, China.Correspondence and requests for materials should be addressed to L.C. (email: chenlang@sustc.edu.cn).

Supplementary Information Outline:

1. Interlayer binding energies and equilibrium distance results

Table 1. Interlayer binding energies (E_{bind}) and equilibrium distances (d) for bilayer graphene, bilayer h-BN, bilayer MoS_2, G/MoS_2 and G/h-BN heterostructures.

Bilayer	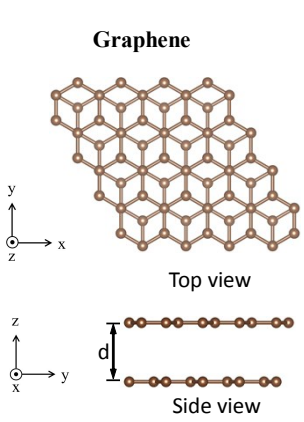		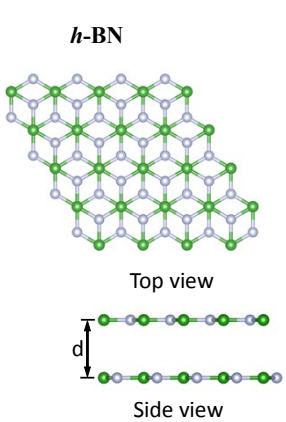		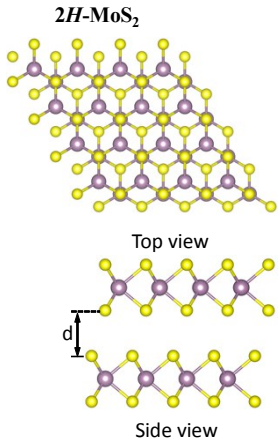	
	E_{bind} (meV/Å^2)	d (Å)	E_{bind} (meV/Å^2)	d (Å)	E_{bind} (meV/Å^2)	d (Å)
D2	19.24	3.247	24.03	3.148	17.10	3.103
OptB88	24.76	3.400	23.17	3.340	25.36	3.094
MBD	17.35	3.472	19.62	3.364	16.77	3.219

G/MoS_2 heterostructure	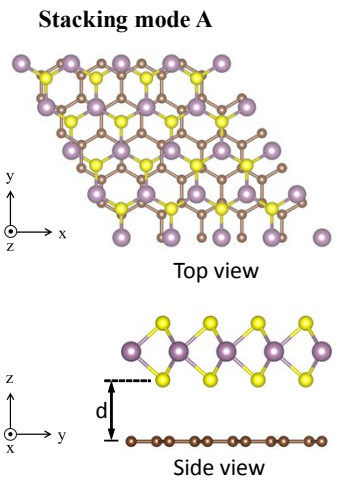		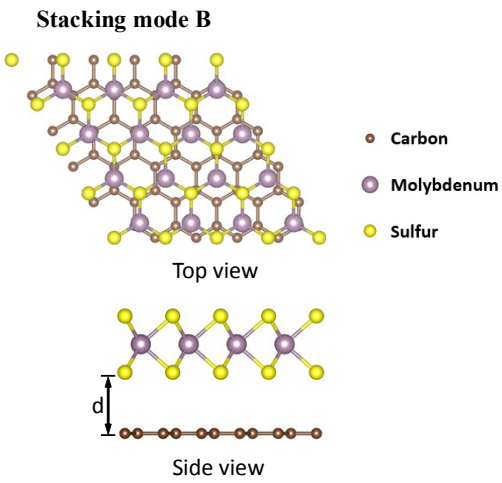	
	E_{bind} (meV/Å^2)	d (Å)	E_{bind} (meV/Å^2)	d (Å)
D2	14.62	3.373	15.17	3.376
OptB88	22.85	3.386	22.84	3.389
MBD	15.96	3.407	15.94	3.411

G/*h*-BN heterostructure	Stacking mode C 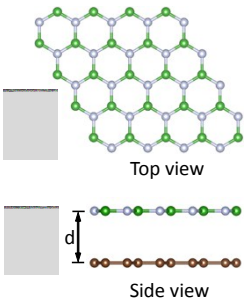		Stacking mode D 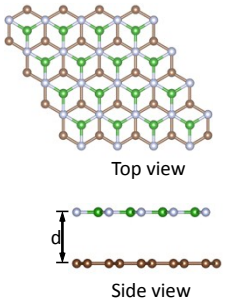		Stacking mode E 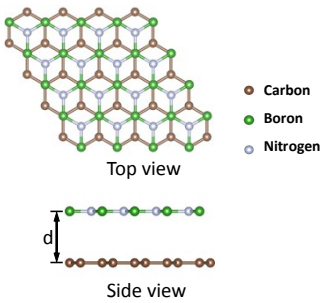	
	E_{bind} (meV/Å^2)	d (Å)	E_{bind} (meV/Å^2)	d (Å)	E_{bind} (meV/Å^2)	d (Å)
D2	17.43	3.366	18.41	3.349	23.26	3.129
OptB88	21.32	3.443	21.93	3.404	25.11	3.327
MBD	16.18	3.577	16.75	3.445	19.61	3.345

2. Out-of-plane Poisson's ratio results

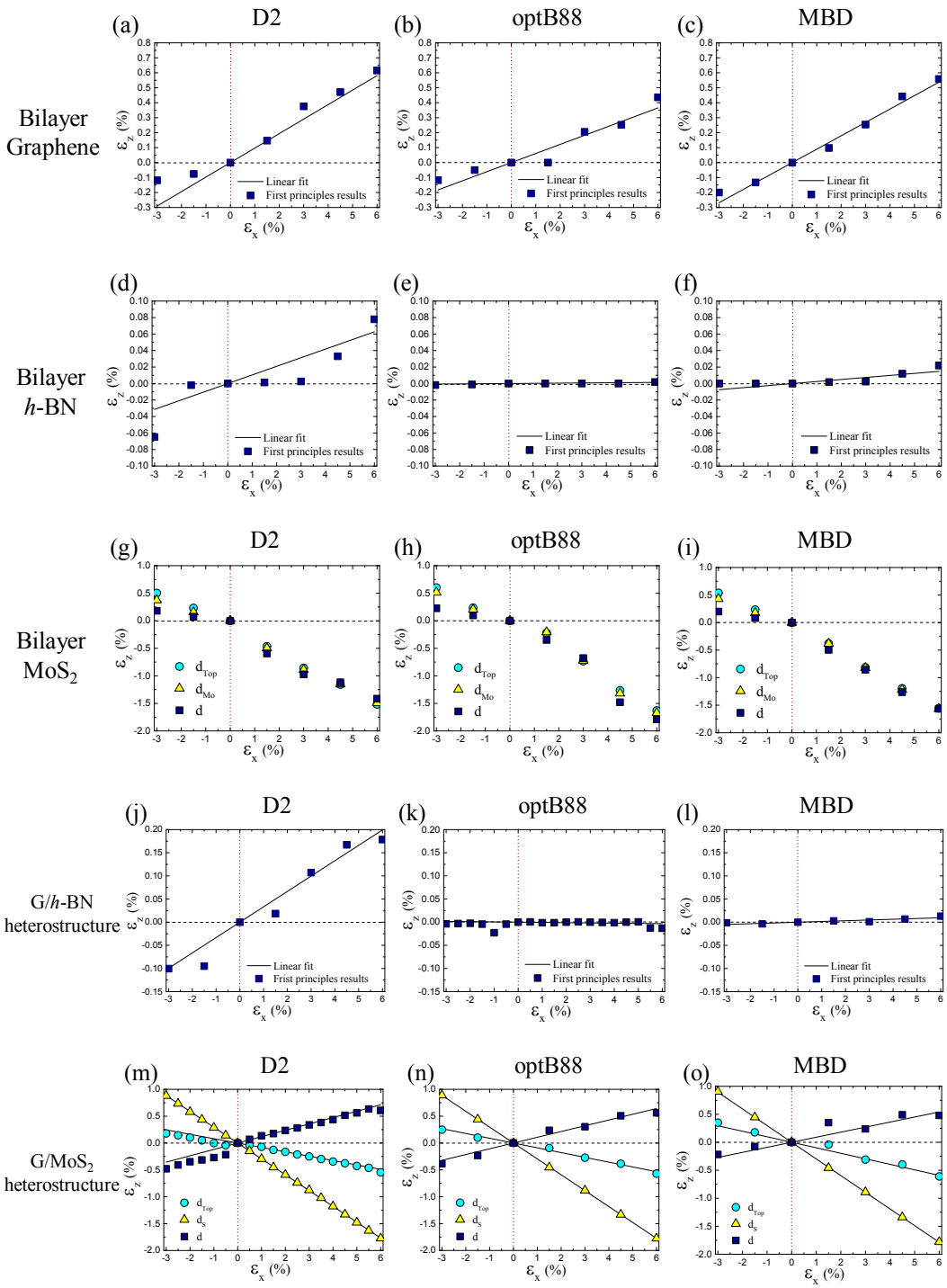

Figure S1. The strain generated in the z direction (ε_z) versus the strain applied in the x direction (ε_x) data of uniaxial deformation of the (**a**, **b**, **c**) bilayer graphene, (**d**, **e**, **f**) bilayer *h*-BN, (**g**, **h**, **i**) bilayer MoS_2, (**j**, **k**, **l**) G/MoS_2 and (**m**, **n**, **o**) G/*h*-BN heterostructures, calculated by density functional theory with different van der Waals corrections.

Table S2. Computational results of out-of-plane Poisson's ratio (ν_{13}) for the bilayer graphene, bilayer *h*-BN, bilayer MoS_2, G/MoS_2 and G/*h*-BN heterostructures by density functional theory with different van der Waals corrections.

		Out-of-plane Poisson's ratio (ν_{13})		
Bilayer		D2	optB88	MBD
Graphene		-0.097	-0.061	-0.089
h-BN		-0.010	-0.00023	-0.0025
MoS_2	d_{Top}	0.247	0.256	0.250
	d_{Mo}	0.240	0.258	0.247
	d	0.228	0.264	0.243
heterostructure				
G/*h*-BN		-0.033	0.0005	-0.002
G/MoS_2	d_{Top}	0.080	0.099	0.089
	d_S	0.295	0.297	0.296
	d	-0.120	-0.090	-0.107

d represents interfacial layer equilibrium distance. d_S represents the distance between S and S atoms. d_{Mo} represents the distance between Mo atoms in upper MoS_2 monolayer and Mo atoms in lower MoS_2 monolayer and d_{Top} represents the distance between top S atoms in upper MoS_2 monolayer and S (C) atoms in lower MoS_2 (Graphene) monolayer (Fig. 1).

3. Out-of-plane Stiffness results

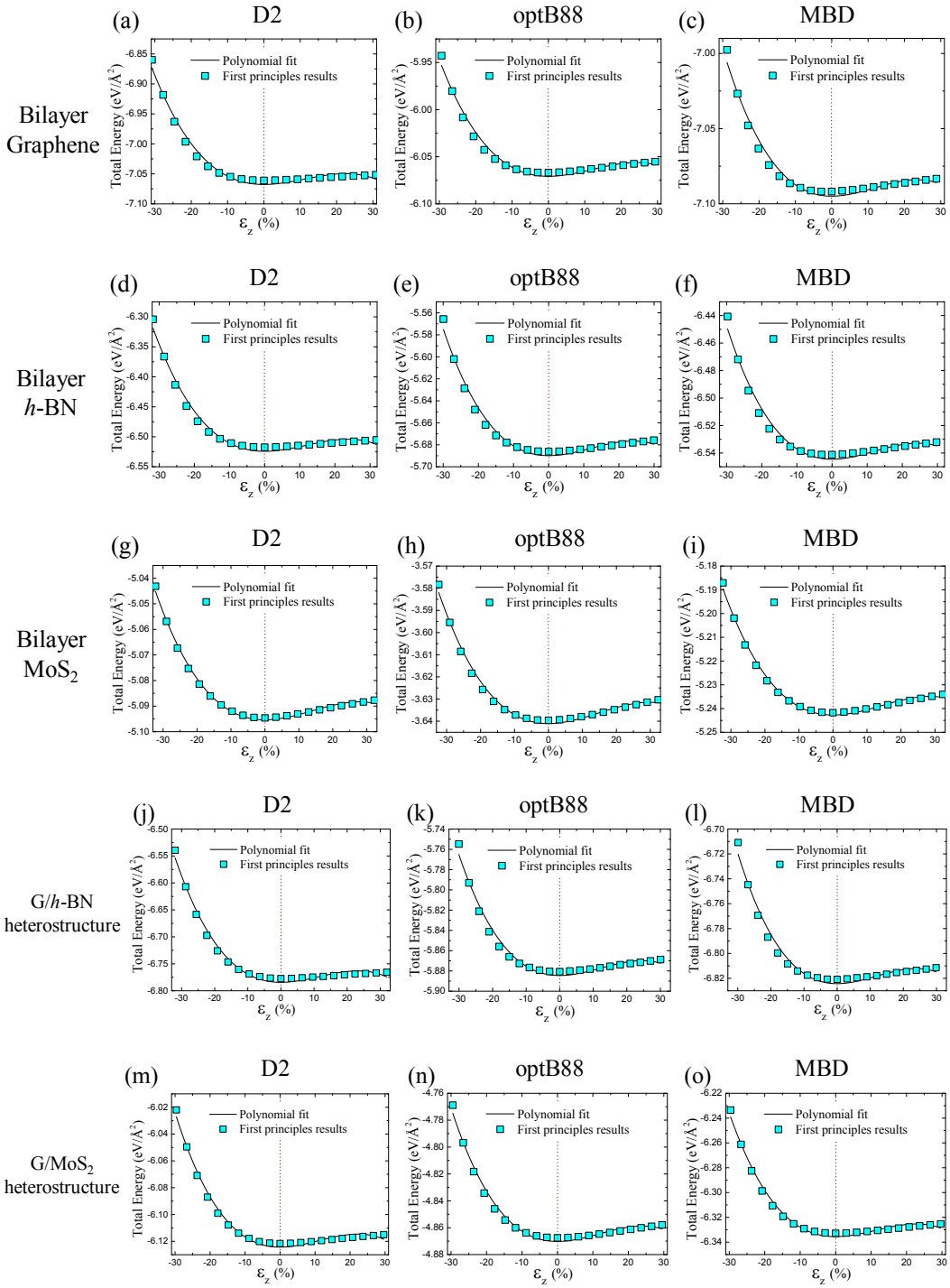

Figure S2. Total energy of the (**a**, **b**, **c**) bilayer graphene, (**d**, **e**, **f**) bilayer *h*-BN, (**g**, **h**, **i**) bilayer MoS_2, (**j**, **k**, **l**) G/MoS_2 and (**m**, **n**, **o**) G/*h*-BN heterostructures with the strain applied in the z direction (ε_z) calculated by density functional theory with different van der Waals corrections.

Table S3. Computational results of out-of-plane stiffness for the bilayer graphene, bilayer *h*-BN, bilayer MoS_2, G/MoS_2 and G/*h*-BN heterostructures by density functional theory with different van der Waals corrections.

	Out-of-plane Stiffness (Gpa)					
Bilayer	D2		optB88		MBD	
	C_{33}	C_{333}	C_{33}	C_{333}	C_{33}	C_{333}
Graphene	106	-939	71	-586	54	-463
h-BN	109	-463	67	-463	56	-463
MoS_2	28	-202	34	-202	30	-210
heterostructure						
G/*h*-BN	121	-1040	70	-571	61	-508
G/MoS_2	56	-500	57	-475	56	-489

4. In-plane Poisson's ratio results

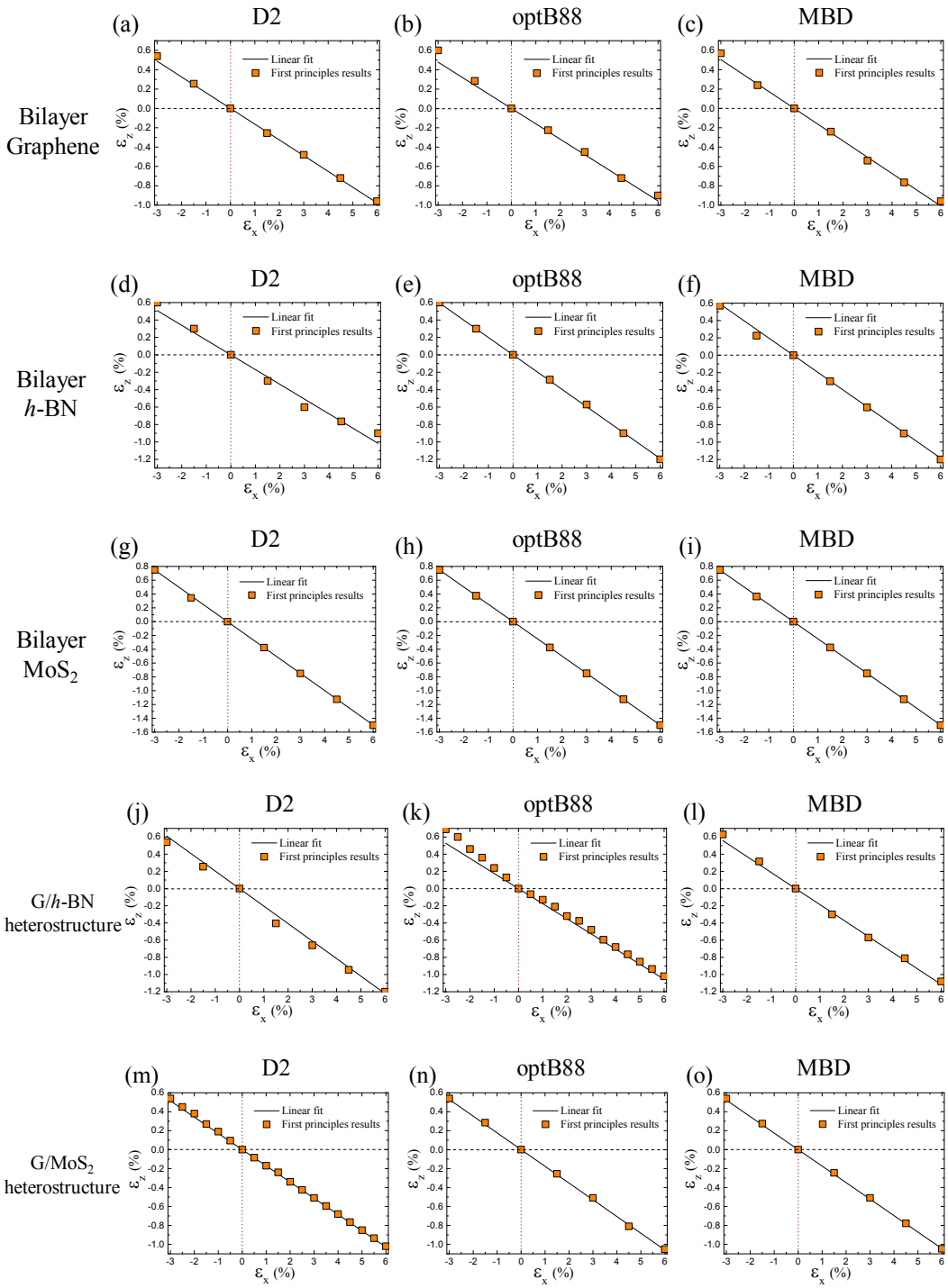

Figure S3. The strain generated in the y direction (ε_y) versus the strain applied in the x direction (ε_x) data of uniaxial deformation of the (**a**, **b**, **c**) bilayer graphene, (**d**, **e**, **f**) bilayer *h*-BN, (**g**, **h**, **i**) bilayer MoS_2, (**j**, **k**, **l**) G/MoS_2 and (**m**, **n**, **o**) G/*h*-BN heterostructures, calculated by density functional theory with different van der Waals corrections.

Table S4. Computational results of in-plane Poisson's ratio (v_{12}) for the bilayer graphene, bilayer *h*-BN, bilayer MoS_2, G/MoS_2 and G/*h*-BN heterostructures by density functional theory with different van der Waals corrections.

	In-plane Poisson's ratio (v_{12})		
Bilayer	D2	optB88	MBD
Graphene	0.163	0.159	0.168
h-BN	0.169	0.199	0.197
MoS_2	0.249	0.250	0.250
heterostructure			
G/*h*-BN	0.204	0.176	0.186
G/MoS_2	0.171	0.177	0.174

5. In-plane Stiffness results

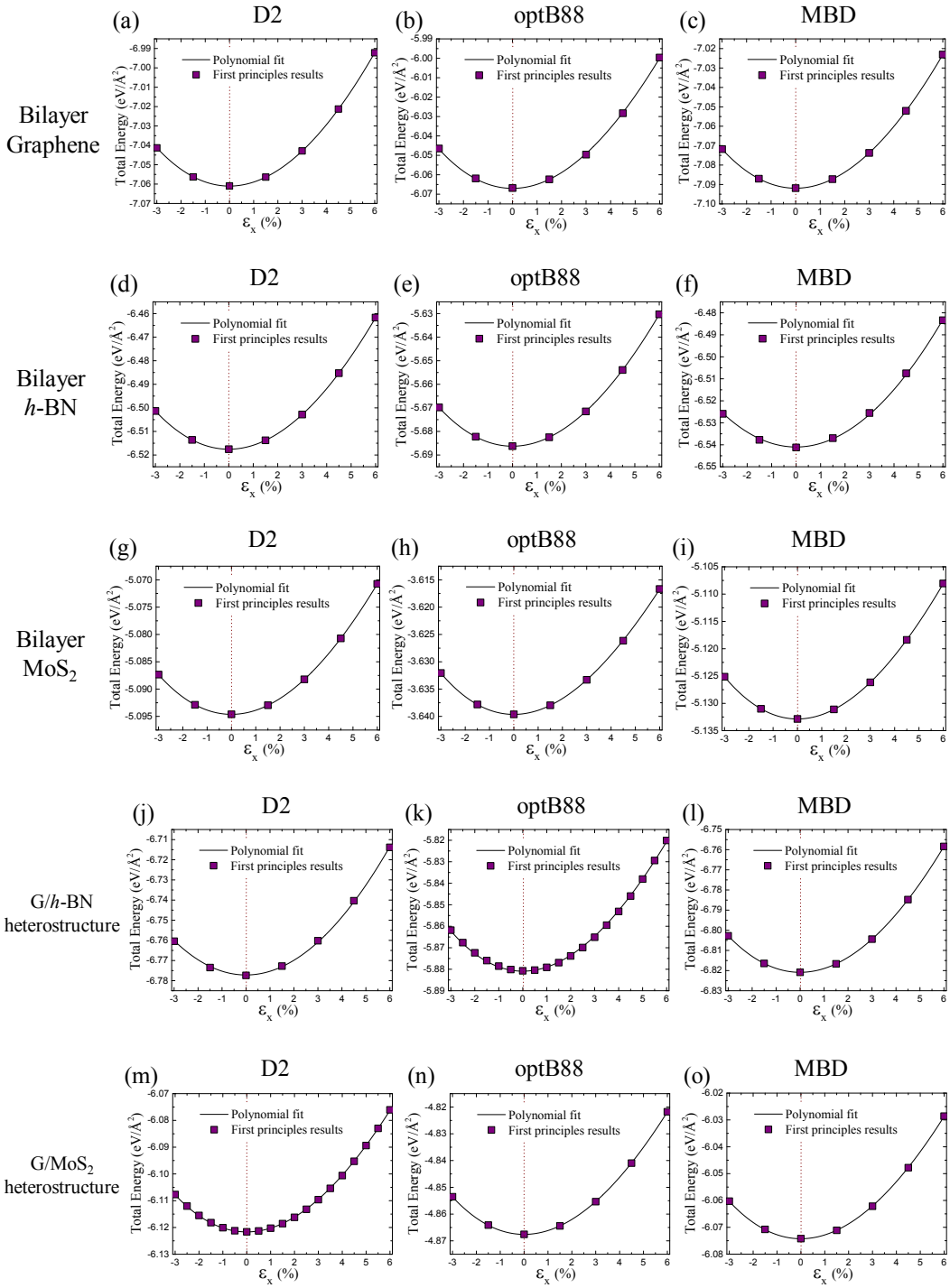

Figure S4. Total energy of the (**a**, **b**, **c**) bilayer graphene, (**d**, **e**, **f**) bilayer *h*-BN, (**g**, **h**, **i**) bilayer MoS_2, (**j**, **k**, **l**) G/MoS_2 and (**m**, **n**, **o**) G/*h*-BN heterostructures with the strain applied in the x direction (ε_x) calculated by density functional theory with different van der Waals corrections.

Table S5. Computational results of in-plane stiffness for the bilayer graphene, bilayer *h*-BN, bilayer MoS_2, G/MoS_2 and G/*h*-BN heterostructures by density functional theory with different van der Waals corrections.

	In-plane Stiffness (Nm^{-1})					
Bilayer	D2		optB88		MBD	
	Y_{11}	Y_{111}	Y_{11}	Y_{111}	Y_{11}	Y_{111}
Graphene	673	-3034	679	-4124	683	-3471
h-BN	551	-2671	554	-2900	538	-1101
MoS_2	244	-1548	247	-2157	256	-1808
heterostructure						
G/*h*-BN	596	-1385	625	-4352	615	-2974
G/MoS_2	465	-2969	468	-3053	465	-3004

By analyzing total energy (see Figure 1), the stiffness (Young's Modulus) SOEC and TOEC of the G/MoS_2 and G/*h*-BN heterostructures in the in-plane direction (Y_{11} and Y_{111}) were derived (see Methods section). The calculated Y_{11} of the G/MoS_2 and G/*h*-BN heterostructures are almost equal to the sum of the stiffness (Young's Modulus) of the two layers of the materials. The Y_{11} of the two-dimensional Graphene, MoS_2, and *h*-BN are 340 Nm^{-1}, 109 Nm^{-1} and 238 Nm^{-1}, respectively[1-3]. This result reveals the reason for the enhanced stability of the carbon-based heterostructures observed in the experiment[4].

6. The relationship between Poisson's ratio and stiffness

The stiffness tensor of a hexagonal crystal system can be written as follows:

$$C_{\alpha\beta} = \begin{pmatrix} C_{11} & C_{12} & C_{13} & 0 & 0 & 0 \\ C_{12} & C_{11} & C_{13} & 0 & 0 & 0 \\ C_{13} & C_{13} & C_{33} & 0 & 0 & 0 \\ 0 & 0 & 0 & C_{44} & 0 & 0 \\ 0 & 0 & 0 & 0 & C_{44} & 0 \\ 0 & 0 & 0 & 0 & 0 & \frac{C_{11} - C_{12}}{2} \end{pmatrix}.$$

The compliance tensor can be obtained by taking inverse of the stiffness tensor:

$$S_{\alpha\beta} = C_{\alpha\beta}^{-1} = \begin{pmatrix} S_{11} & S_{12} & S_{13} & 0 & 0 & 0 \\ S_{12} & S_{11} & S_{13} & 0 & 0 & 0 \\ S_{13} & S_{13} & S_{33} & 0 & 0 & 0 \\ 0 & 0 & 0 & S_{44} & 0 & 0 \\ 0 & 0 & 0 & 0 & S_{44} & 0 \\ 0 & 0 & 0 & 0 & 0 & 2(S_{11} - S_{12}) \end{pmatrix}.$$

The in-plane Poisson's ratio v_{12} and the out-of-plane Poisson's ratio v_{13}:

$$\begin{cases} v_{12} = -\dfrac{S_{12}}{S_{11}} \\ v_{13} = -\dfrac{S_{13}}{S_{11}}. \end{cases}$$

After simplification,

$$\begin{cases} v_{12} = \dfrac{{C_{13}}^2 - C_{12}C_{33}}{{C_{13}}^2 - C_{11}C_{33}} \\ v_{13} = \dfrac{C_{13}(C_{12} - C_{11})}{{C_{13}}^2 - C_{11}C_{33}}. \end{cases}$$

Therefore, we can verify the accuracy of the results by the relationship between Poisson's ratio and stiffness tensor.

7. the relationship between θ and ν_{13}

When i fixed in the x direction and j varying in the y-z plane by an angle of θ, the transformation from the stress σ_β (unprimed) to the stress $\sigma_{\beta'}$ in arbitrary system (primed) is described by:

$$\underbrace{\begin{pmatrix}\sigma_{1'}\\ \sigma_{2'}\\ \sigma_{3'}\\ \sigma_{4'}\\ \sigma_{5'}\\ \sigma_{6'}\end{pmatrix}}_{\breve{\sigma}_{\beta'}} = \underbrace{\begin{pmatrix}1 & 0 & 0 & 0 & 0 & 0\\ 0 & \cos^2\theta & \sin^2\theta & 2\sin\theta\cos\theta & 0 & 0\\ 0 & \sin^2\theta & \cos^2\theta & -2\sin\theta\cos\theta & 0 & 0\\ 0 & -\sin\theta\cos\theta & \sin\theta\cos\theta & \cos^2\theta-\sin^2\theta & 0 & 0\\ 0 & 0 & 0 & 0 & \cos\theta & -\sin\theta\\ 0 & 0 & 0 & 0 & \sin\theta & \cos\theta\end{pmatrix}}_{\breve{T}_{\sigma_{\beta'\beta}}} \underbrace{\begin{pmatrix}\sigma_1\\ \sigma_2\\ \sigma_3\\ \sigma_4\\ \sigma_5\\ \sigma_6\end{pmatrix}}_{\breve{\sigma}_\beta}.$$

Note that we use contracted notations (11→1, 22→2, 33→3, 13→4, 23→5, 12→3, $C_{ijkl}\rightarrow C_{\alpha\beta}$, $C_{ijklmn}\rightarrow C_{\alpha\beta\gamma}$) for the tensor indices. The transformation from the strain ε_α (unprimed) to the strain $\varepsilon_{\alpha'}$ in arbitrary system (primed) is described by:

$$\underbrace{\begin{pmatrix}\varepsilon_{1'}\\ \varepsilon_{2'}\\ \varepsilon_{3'}\\ \varepsilon_{4'}\\ \varepsilon_{5'}\\ \varepsilon_{6'}\end{pmatrix}}_{\breve{\varepsilon}_{\alpha'}} = \underbrace{\begin{pmatrix}1 & 0 & 0 & 0 & 0 & 0\\ 0 & \cos^2\theta & \sin^2\theta & \sin\theta\cos\theta & 0 & 0\\ 0 & \sin^2\theta & \cos^2\theta & -\sin\theta\cos\theta & 0 & 0\\ 0 & -2\sin\theta\cos\theta & 2\sin\theta\cos\theta & \cos^2\theta-\sin^2\theta & 0 & 0\\ 0 & 0 & 0 & 0 & \cos\theta & -\sin\theta\\ 0 & 0 & 0 & 0 & \sin\theta & \cos\theta\end{pmatrix}}_{\breve{T}_{\varepsilon_{\alpha'\alpha}}} \underbrace{\begin{pmatrix}\varepsilon_1\\ \varepsilon_2\\ \varepsilon_3\\ \varepsilon_4\\ \varepsilon_5\\ \varepsilon_6\end{pmatrix}}_{\breve{\varepsilon}_\alpha}.$$

The compliance coefficients $S_{\alpha'\beta'}$ are defined as the proportionality constants between stress $\sigma_{\beta'}$ and strain by the Hooke's law:

$$\varepsilon_{\alpha'} = S_{\alpha'\beta'}\sigma_{\beta'}.$$

It can be expressed by the coordinate transformation equation:

$$T_{\varepsilon_{\alpha'\alpha}}\varepsilon_\alpha = S_{\alpha'\beta'}T_{\sigma_{\beta'\beta}}\sigma_\beta.$$

We obtain

$$\varepsilon_\alpha = \underbrace{T_{\varepsilon_{\alpha'\alpha}}^{-1}S_{\alpha'\beta'}T_{\sigma_{\beta'\beta}}}_{\breve{S}_{\alpha\beta}}\sigma_\beta,$$

and

$$S_{\alpha'\beta'} = T_{\varepsilon_{\alpha'\alpha}}S_{\alpha\beta}T_{\sigma_{\beta'\beta}}^{-1}.$$

The out-of-plane Poisson's ratio ν_{13}:

$$v_{13} = -\frac{S_{13}}{S_{11}}.$$

After simplification,

$$v_{13}(\theta) = -\frac{(C_{11} - C_{12})C_{13}\cos^2\theta - \left({C_{13}}^2 - C_{12}C_{13}\right)\sin^2\theta}{{C_{13}}^2 - C_{11}C_{13}}.$$

Reference

1. N. G. Chopra and A. Zettl, *Solid State Communications*, 1998, **105**, 297-300.

2. S. Woo, H. C. Park and Y.-W. Son, *Phys. Rev. B*, 2016, **93**, 075420.

3. M. de Jong, W. Chen, T. Angsten, A. Jain, R. Notestine, A. Gamst, M. Sluiter, C. Krishna Ande, S. van der Zwaag, J. J. Plata, C. Toher, S. Curtarolo, G. Ceder, K. A. Persson and M. Asta, *Sci. Data.*, 2015, **2**, 150009.

4. C.-M. Park and H.-J. Sohn, *Adv. Mater.*, 2007, **19**, 2465-2468.